Metamaterials : opportunities in medical imaging.

R. Abeddaim[a], P. Lecoq[b] and S. Enoch*[a]
[a]Aix-Marseille Université, CNRS, Centrale Marseille, Institut Fresnel, UMR 7249, 13013 Marseille, France
[b]Conseil Européen pour la Recherche Nucléaire (CERN), 1211 Genève, Switzerland;

ABSTRACT

Metamaterials are a highly topical field of modern physics that has created new exciting technological opportunities in many areas, including medical imaging and sensor developments. Managing near-field light-matter interactions at a subwavelength scale provides new avenues to develop efficient antennas and detectors.

Metamaterials have been proposed as a potential solution to control emission or conversion of light for more than a decade. The Near Zero Index metamaterials have been proposed to design directive emitters. More recently so-called hyperbolic metamaterials have been intensively studied. These structures possess effective permeability or permittivity tensors components such that one principal component is opposite to the two others.

With the example of coils for Ultra-High field magnetic resonance imaging and positron emission tomography we will show how medical imaging could benefit from such control of the electromagnetic waves.

Keywords: metamaterials, medical imaging, MRI, PET

1. INTRODUCTION

Medical imaging includes anatomical imaging such as X-Ray tomography or magnetic resonance imaging (MRI) but also functional imaging methods such as Positron Emission Tomography that could provide information about physiologic function. Progress in Medical Imaging are always expected to provide better diagnosis. Medical imaging is also key technology for the field of personalized medicine [1].

From an engineering point of view, information collected by the medical imaging devices rely on waves, that could be acoustic waves (ultrasound scans), X-Rays (CT), radiofrequency waves (MRI), optical photons and gamma photons (PET) for example. Thus, physics and engineering of the control of waves are of tremendous interest for medical imaging.

Metamaterials have been subject of intensive research since the beginning of the millennium. The seminal paper by Sir John Pendry [2, 3] is often considered as the starting point that aroused the interest of researchers for this topic. In this paper he shows that a slab of material whose relative permittivity and permeability are equal to -1 acts as a perfect lens, that is a lens that is not restrained by the Rayleigh resolution limit. These materials are also known as negative index materials. Although such material doesn't exist in nature periodic arrangement of copper wires and split ring resonators could mimic the desired properties [4].

Thus, metamaterials are usually defined as composite materials whose effective properties cannot be obtained from natural homogeneous materials. Besides negative index material many properties could be obtained such as near zero index materials [5,6], extreme anisotropy…

In this paper, we illustrate how metamaterials could be useful for improving medical imaging with two examples: Ultra High Field MRI (UHF MRI) and Positron Emission Tomography (PET).

2. ULTRA HIGH FIELD MRI

MRI is one of the most attractive imaging modality as it combines many interesting characteristics. First it doesn't involve ionizing rays (such as X-Rays) or injections of tracers (such as PET). In addition it provides anatomic images

but can also provide functional images. Thus, MRI is unique in providing this amount of information on the investigated imaging subject.

MRI is based on the presence of a strong magnetic field (B_0) that causes energy levels of nuclei of specific atoms to split. By applying a radio-frequency (RF) field with frequency corresponding to the so-called Larmor frequency, atomic nuclei are excited into a higher energy state. When relaxing, the nuclei emit signals with the same RF frequency as the one picked up by the system and is processed into an image. Both transmitted and received RF fields are called B_1 fields. Note that the most important chemical element to image is hydrogen with, for example, a Larmor frequency of 64 MHz for 1.5 Tesla systems.

In recent decades, there has been a constant drive to pursue ever-increasing field strengths. Higher magnetic field strengths provide more signals, resulting in better quality images. The increase of the static field is not only justified by the fact that it allows better resolution and reduced acquisition times, but it also offers the possibility to evidence structures and details impossible to visualize at lower field. Several studies have already shown the potential of UHF MRI in a clinical context to improve patient care. This explains the development of MRI research machines at high and ultrahigh-field (equal to or greater than 7 Tesla) on the international scene. Currently, most of MRI clinical scanners in the world have a B0 static field of 1.5Tesla and 3 Tesla. An increasing number of institutes are exploring the use of 7Tesla systems with a couple of institutes having systems of 9.4, 10.5 or even 11.7 Tesla. However, the higher magnetic field strength comes with a higher Larmor frequency. At 7 Tesla, the Larmor frequency has reached 300 MHz and at 11.7T the frequency of the B_1 field has even reached 500 MHz. The increase of this frequency has a series of disadvantageous consequences that are causing an apparent reduction of the benefit of ultrahigh field MRI. At ultrahigh fields, the increased frequency corresponds to smaller wavelength. At 7 Tesla, the wavelength becomes smaller than the cross-sectional dimensions of the human body. This results in standing wave patterns in the B_1 field distribution, with regions of destructive interference, depending on the imaging subject and the RF coil array. In addition, any RF distribution will deposit energy, like in a microwave oven. The energy deposition is a spatially inhomogeneous distribution, expressed as the local specific absorption ratio (SAR). The SAR levels increase with frequency. In addition, at ultrahigh field strengths, the SAR distribution is becoming more and more heterogeneous. To avoid tissue heating, the duty cycle of the MRI experiment must be sufficiently low so the maximum local SAR level remains below predefined thresholds.

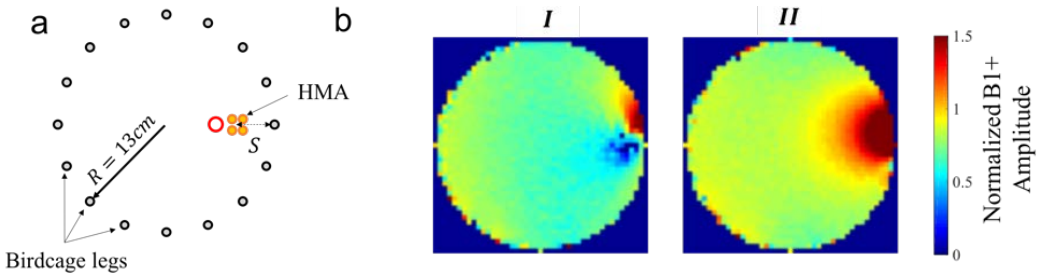

Figure 1: magnetic field control inside a birdcage using HMA, a sketch of the setup, b1 second Kerker condition, b2 first Kerker condition

Thus, B_1 homogeneity in 7T MRI remains an important challenge in ultra-high field MRI scanners. Passive shimming using High-dielectric constant pads have been proposed and optimized to overcome these issues [8-10]. Common formulations of dielectric pads for 7T applications are based on $BaTiO_3$ mixed with water present some drawbacks such as performance decay over time. While previous studies tackled directly the formulation problem introducing new dielectric materials and solvent [11], we proposed a new approach based on metamaterial [12]. Our approach is based on the so called Kerker effect [13]. This effect allows to tailor simultaneously the electric and magnetic responses of a single dielectric particle. This Kerker scattering conditions can be achieved by using several resonant elements to build up a more complex unit cell using coupling mechanism [14]. The meta atom considered here is based on a set of four hybridized resonant metallic wires (see Fig. 1). It will be referred as hybridized meta atom (HMA). The HMA is placed inside a birdcage coil. A sketch of the considered geometry is presented in Fig 1.

When the HMA is insert inside the birdcage we observe an increase of B_1^+ field in the phantom on the right, i.e. near the HMA. This effect is related to the increase of the local magnetic field when a resonant mode is excited. When the length is further tuned to rich the second Kerker condition, we are able to decrease drastically the B_1^+ field when the backward scattering condition is reached at a length equal to 49 cm. Then, we observe an even stronger increase in the near B_1^+ field at the forward scattering condition length (49.5 cm).

Besides this results many other application of metamaterials are of interest for MRI systems. Some of them could be found on M-Cube project website [15]

3. POSITRON EMISSION TOMOGRAPHY

Since the seventies, positron emission tomography (PET) has become an invaluable medical molecular imaging modality, especially for cancer diagnosis and the monitoring of its response to therapy and more recently in direct combination with X-ray computed tomography (CT) or magnetic resonance (MR).

PET is an incredibly sensitive imaging technique based on electron-positron annihilations and the nearly coincident detection of the corresponding pairs of photons simultaneously emitted in opposite directions and electronically collimated along a common line, *aka.* a line of response (LOR). Accumulated detections of different annihilation events along various LORs produce projections of the radioactive concentration volume distribution of a radiopharmaceutical labelled with a positron emitter radioisotope, such as ^{18}F or ^{11}C. Tomographic image reconstruction from all the measured projections then leads to the 3D volume representation of the estimated radionuclide distribution, whose accuracy depends mainly on the ability to associate coincident detections with actual annihilation photons.

As shown in Fig. 2, the localization of the emission point of an annihilation pair along a LOR depends on the detection of the time difference between the two annihilation photons, also known as the time-of-flight (TOF) difference of the photons, whose accuracy is given by the coincidence time resolution (CTR). This additional information makes the tomographic inversion problem much less ill-posed, hence resulting in a better signal-to-noise ratio of the activity measurement. Taking-into-account the speed of light, which is approximately 30 cm/ns, a CTR better than 10 picoseconds FWHM will ultimately allow to obtain a direct 3D volume representation of the estimated activity distribution of a positron emitting radiopharmaceutical, at the mm level and without the need for tomographic inversion, thus introducing a quantum leap in PET imaging and quantification.

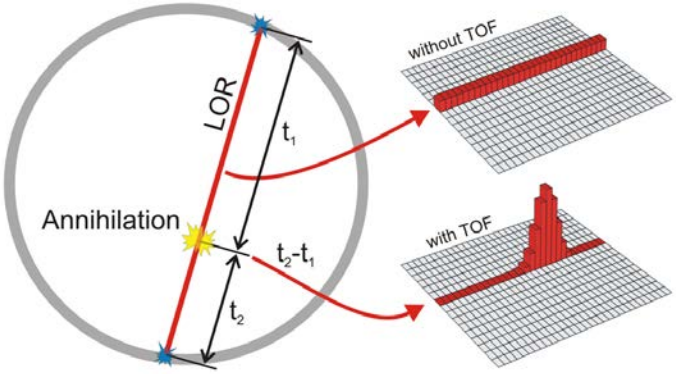

Fig.2: Principle of Time-of-Flight PET scanner

Moreover, a 10 ps capability will increase the effective PET sensitivity through a significant increase of the image signal-to-noise ratio, as compared to the state-of-the-art, by at least a factor of 16, with the following expected consequences:

- Reduction of the radiation doses of molecular imaging procedures to negligibly low levels;
- Reduction of the synthesized quantity of radiopharmaceutical needed for each examination, and thus of the relatively high cost currently associated with in-vivo molecular imaging procedures;

- Further extension of the benefit of molecular imaging procedures beyond oncology and towards cardiovascular, neurological, metabolic, inflammatory, infectious or metabolic disease (such as diabetes), including in the paediatric, neonatal, and prenatal contexts;
- Precise dynamic studies of molecular processes of high interest in pharmacology for screening and selecting candidate molecules for the next generation of drugs or new applications thereof;
- Potentially further extension of molecular in-vivo imaging to study "systems biology" of the whole human body through whole-body imaging systems;
- No need for full angular coverage of the patient, opening many new opportunities for PET system design, in particular for organ-specific devices.

While crossing the **10 ps frontier** will increase the performance of TOF-PET and lead to the advent of reconstruction-less PET, it will also permit efficient positron range monitoring in hadrontherapy (with protons and carbon), improve the performance of Compton camera developed for conventional scintigraphy and nuclear waste management, and impact both the development of positron annihilation lifetime spectroscopy (PALS) used in material science and the development of laser imaging detection and ranging (LIDAR) systems for automotive solutions, e.g. for self-driving cars. Such a feat will not only require to make progresses on the development of new scintillators (*e.g.* to produce enough photons with a minimum time jitter in the first 10 ps after their excitation), but also on markedly improving light collection, photo-detection and photo-detector electronic readout.

Standard scintillation mechanisms are unlikely to generate a high enough photon rate to access the 10 ps range time resolution at low energy of gamma rays produced via positron decay (511 keV). However, the production of prompt photons, in addition to the scintillation pulse, even in relatively small numbers (a few hundreds) would significantly improve the time resolution [16].

Among the possible sources of prompt photons, the Cerenkov effect must be considered.
Another possible way to produce prompt photons is to develop hetero-structures based on a combination of standard scintillators (such as LSO, LYSO, BGO) and nanocrystals. Nanocrystals have gained considerable attention over the last two decades because of their excellent fluorescence properties. In such systems quantum confinement offers very attractive properties, among which a very high quantum efficiency and ultrafast decay time. Moreover, they have a broadband absorption and narrow emission, enhanced stability compared to organic dyes, and the fluorescence is essentially tunable from the UV, over the visible, to the near-infrared spectral range (300 nm – 3000 nm) by nanocrystal size and material composition.

High quality semiconductors, e.g. GaAs or CdSe, based on nano-structures have a light yield that can reach 70-80% of absorbed energy as compared to at most 15% in standard scintillators such as LSO or $LaBr_3$. Moreover, the emission lifetime is usually shorter than 1ns. These impressive performances are attributed to electron confinement, phonon confinement and optical resonances taking place in these nano-materials. Embedded in meta-structures based on polymers or heavy scintillators (such as LSO, LYSO or heavy scintillating glasses) they could complement the standard scintillation signal with a very fast light component that could be exploited for reaching an ultimate timing resolution.
Bright and transparent ZnO:Ga polystyrene composites prepared by homogeneous embedding of ZnO:Ga nanocrystals into a scintillating organic matrix have shown an ultrafast subnanosecond luminescence, as seen on Fig. 3 [17].

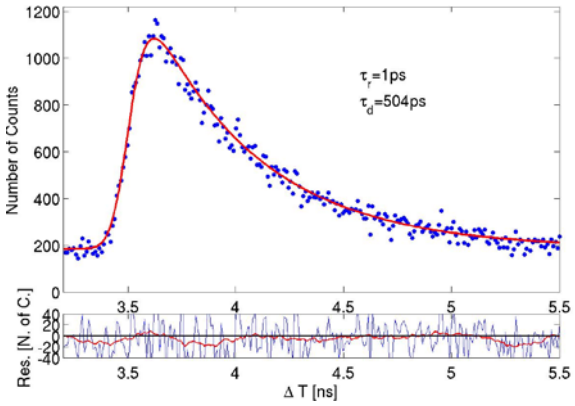

Fig. 3: Pulse shape of 1mm thick polystyrene slab with 10 wt% of ZnO:Ga nanocrystals under picosecond X-Ray excitation

Colloidal CdSe nano-sheets (CQwells), a new class of two-dimensional materials. Ref. [18] offer another route toward the realization of ultrafast timing resolution. CQwells are solution-processed analogs to epitaxial quantum wells (Qwells), but because they are synthesized in solution, they can be deposited on any substrate with any geometrical configuration. Further, a large dielectric mismatch between the inorganic CdSe CQwells and the surrounding organic environment results in much stronger quantum confinement than in epitaxial Qwells. This mismatch combined with very little dielectric screening due to the 1.5 nm CQwell thickness results in strongly enhanced exciton and bi-exciton (bound state of two excitons) binding energies of 132 and 30meV, respectively, making both populations stable at room temperature.

The strong electron and hole confinement in one dimension and free motion in the plane has several important consequences, including strict momentum conservation rules (in contrast to quantum dots) and a giant oscillator strength transition. Momentum conservation in CQwells limits the available states for Auger transitions, reducing the recombination rate of this non-radiative channel. In addition to the enhanced exciton and bi-exciton binding energies, a giant oscillator transition results in radiative lifetimes that are significantly shorter than in bulk CdSe (~400 and ~100ps, respectively). All of these properties contribute to the ultralow threshold for stimulated emission (or super-luminescence) with sub-ps rise time and sub-ns decay time that have been observed with these CQwells and described in [19]. Streak camera images are shown in Fig. 4. Such systems could find interesting application in ultrafast X-Ray imaging as well as for providing a fast time tag in γ imaging if used in hetero-structures in combination with dense scintillators like LSO with a structuration dimension of the order of the recoil electron range, as suggested in Ref [20] and shown in Fig. 5 from [21].

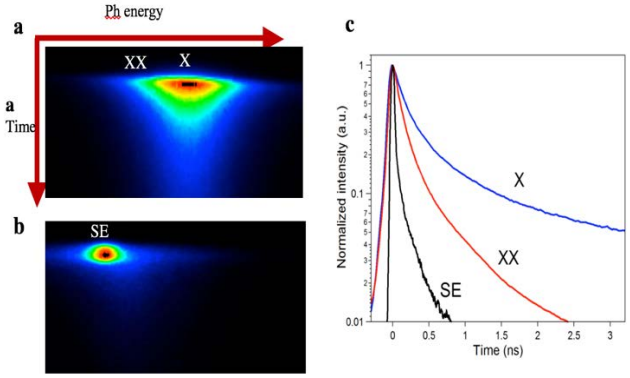

Fig. 4: Time-resolved spectral decay under femtosecond excitation (a) Streak image showing the spectral decay of exciton (X) and bi-exciton (XX) emission from CdSe CQwells. (b) Stimulated emission of a very low excitation fluence (6μJ/cm^2), with characteristic spectral narrowing and lifetime shortening. (c) Decay time curves of exciton (X), bi-exciton (XX) and stimulated emission SE.

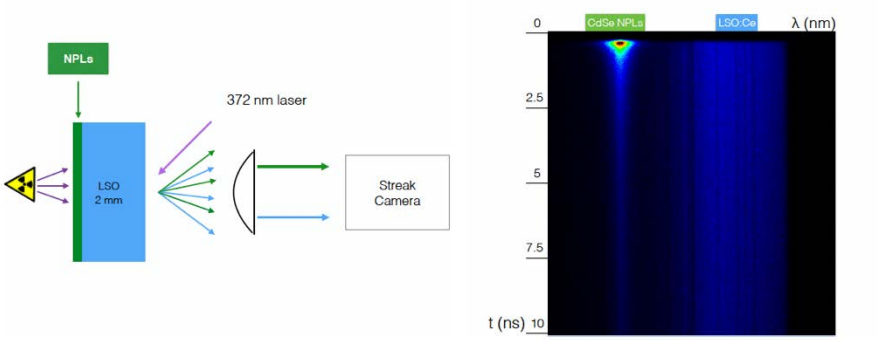

Fig. 5. Example of an hetero-structure made of a 2mm thick slab of LSO crystal with a 100µm layer of CdSe nano-sheets excited by a pulsed X-ray source. The streak camera image at the bottom shows on a vertical 10ns scale the long LSO scintillation centered at 420nm and the much shorter sub-ns emission from the CdSe CQwells at 530nm. The long tail at 530nm corresponds to the CQwell emission under excitation by the LSO scintillation light (from [20]).

AKNOWLEDGMENTS

The project leading to this publication has received funding from Excellence Initiative of Aix-Marseille University–A*MIDEX, a French “Investissements d’Avenir” programme. It has been partly funded by France Life Imaging Grant No. ANR-11-INBS-0006. It has received funding from the European Union’s Horizon 2020 Research and Innovation program under Grant Agreement No. 736937. We also thank Institut Carnot STAR for support.

One of the authors (PL) has received the support from CERN and from the European Research Council for the ERC Advanced Grant TICAL #338953

REFERENCES

[1] European Society of Radiology (ESR). Medical imaging in personalized medicine: a white paper of the research committee of the European Society of Radiology (ESR). Insights Imaging. 6(2):141–155. doi:10.1007/s13244-015-0394-0, (2015)
[2] Pendry, J. B. Negative refraction makes a perfect lens. Physical review letters, 85(18), 3966. (2000).
[3] Veselago, V. G. Electrodynamics of substances with simultaneously negative and. Usp. Fiz. Nauk, 92, 517. (1967).
[4] Shelby, R. A., Smith, D. R., & Schultz, S. Experimental verification of a negative index of refraction. science, 292(5514), 77-79. (2001).
[5] Enoch, S., Tayeb, G., Sabouroux, P., Guérin, N., & Vincent, P. A metamaterial for directive emission. Physical Review Letters, 89(21), 213902. (2002).
[6] Liberal, I., & Engheta, N. Near-zero refractive index photonics. Nature Photonics, 11(3), 149. (2017).
[7] Poddubny, A., Iorsh, I., Belov, P., & Kivshar, Y. Hyperbolic metamaterials. Nature photonics, 7(12), 948. (2013).
[8] Webb, A. G. Dielectric materials in magnetic resonance. Concepts in magnetic resonance part A, 38(4), 148-184. (2011).
[9] O’Reilly, T. P. A., Webb, A. G., & Brink, W. M. Practical improvements in the design of high permittivity pads for dielectric shimming in neuroimaging at 7 T. Journal of Magnetic Resonance, 270, 108-114. (2016).

[10] Neves, A. L., Leroi, L., Raolison, Z., Cochinaire, N., Letertre, T., Abdeddaïm, R., ... & Malléjac, N. Compressed perovskite aqueous mixtures near their phase transitions show very high permittivities: New prospects for high-field MRI dielectric shimming. Magnetic resonance in medicine, 79(3), 1753-1765. (2018).
[11] Z. Raolison, et al., Proc. Intl. Soc. Mag. Reson. Med., Paris, France, 26, 2664 (2018)
[12] Dubois, M., Leroi, L. Raolison, Z., Abdeddaim, R., Antonakakis, T., de Rosny, J. Vignaud, A., Sabouroux, P., Georget, E. , Larrat, B., Tayeb, G., Bonod, N., Amadon, A., Mauconduit, F., Poupon, C., Le Bihan, D., Enoch, S. Kerker effect in ultrahigh-field magnetic resonance imaging. Physical Review X, 8(3), 031083. (2018).
[13] M. Kerker, D.S. Wang and C.L. Gilles, "Electromagnetic scattering by magnetic spheres", JOSA, vol. 73, pp. 765-767, (1983).
[14] N. Meinzer, W.L. Barnes, and I.R. Hooper, "Plasmonic meta-atoms and metasurfaces", Nature Photonics, vol. 8, pp. 889-898, (2014).
[15] M-Cube website : http://www.mcube-project.eu/
[16] P. Lecoq, "Pushing the limits in Time-Of-Flight PET imaging", IEEE TRANSACTIONS ON RADIATION AND PLASMA MEDICAL SCIENCES, VOL. 1, NO. 6, NOVEMBER (2017)
[17] H. Buresova et al., "Preparation and luminescence properties of ZnO :Ga – polystyrène composite scintillator", Optics express, Vol. 24, No. 14, OPTICS EXPRESS 15289. (2016)
[18] J.Q. Grim et al., "Continuous-Wave Biexciton Lasing at Room Temperature Using Solution-Processed Quantum Wells" Nat. Nanotechnol. 9, 891–895 (2014).
[19] Lehmann W (1966) Edge emission of n-type conducting ZnO and CdS. Solid-State Electronics 9: 1107–1110
[20] P. Lecoq, "Metamaterials for novel X- or g-ray detector designs", 2008 IEEE Nuclear Science Symposium Conference Record, N07-1, pp.680-684.
[21] Turtos RM et al, Ultrafast emission from colloïdal nanocrystals under pulsed X-ray excitation. JINST_068P_06. (2016).